

Discovery of 4-Aryl-2-benzoyl-imidazoles as Tubulin Polymerization Inhibitor with Potent Antiproliferative Properties

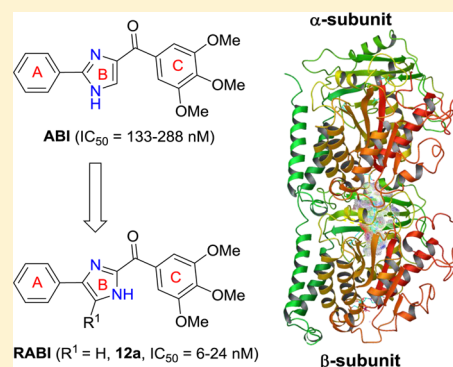
Min Xiao,^{†,§} Sunjoo Ahn,^{‡,§} Jin Wang,[†] Jianjun Chen,[†] Duane D. Miller,^{†,‡} James T Dalton,[‡] and Wei Li^{*,†}

[†]Department of Pharmaceutical Sciences, University of Tennessee Health Science Center, Room 327B, 847 Monroe Avenue, Memphis, Tennessee 38163, United States

[‡]GTx, Inc., Memphis, Tennessee 38163, United States

S Supporting Information

ABSTRACT: A series of 4-aryl-2-benzoyl-imidazoles were designed and synthesized based on our previously reported 2-aryl-4-benzoyl-imidazole (ABI) derivatives. The new structures reversed the aryl group and the benzoyl group of previous ABI structures and were named as reverse ABI (RABI) analogues. RABIs were evaluated for biological activity against eight cancer cell lines including multidrug-resistant cancer cell lines. In vitro assays indicated that several RABI compounds had excellent antiproliferative properties, with IC_{50} values in the low nanomolar range. The average IC_{50} of the most active compound **12a** is 14 nM. In addition, the mechanism of action of these new analogues was investigated by cell cycle analysis, tubulin polymerization assay, competitive mass spectrometry binding assay, and molecular docking studies. These studies confirmed that these new RABI analogues maintain their mechanisms of action by disrupting tubulin polymerization, similar to their parental ABI analogues.



INTRODUCTION

Cancer remains one of the leading causes of mortality worldwide.^{1,2} While current therapies are effective in treating early stage cancers, the efficacy against advanced cancers, especially multidrug-resistant cancers, is limited. Thus, developing novel anticancer agents that can effectively overcome multidrug resistance will provide significant improvement of quality of life in cancer patients.

We previously reported the discovery of ABI analogues targeting the colchicine binding site in tubulin as potent antiproliferative agents.^{3–8} Compared with existing tubulin-targeting agents such as paclitaxel, colchicine, or vinblastine, ABI compounds have comparable in vitro and in vivo potency but can effectively circumvent several clinically relevant multidrug resistant mechanisms, including drug resistance mediated by P-glycoprotein (Pgp), multidrug resistance-associated proteins (MRPs), and breast cancer resistant proteins (BCRP).^{5,6} ABI compounds have also shown excellent oral bioavailability,⁵ a potential advantage over existing tubulin inhibitors which can only be administered by intravenous injection. To further optimize the potency of ABI analogues and to gain further insight in their structure–activity relationships (SARs), we designed and synthesized several new series of ABI analogues (summarized in Figure 1) by introducing three major changes to the parental ABI scaffold as described below.

First, we varied the substitutions at the para-position on the A ring of ABI analogues. This was accomplished by using previously established synthetic strategies.^{3,4,7} Second, we

reversed the two major substitutions on the B ring to produce the 4-aryl-2-benzoyl-imidazoles (reverse ABI, or RABI) compounds. We developed a one-pot synthetic strategy to synthesize RABI analogues in good yields based on the literature for synthesizing similar scaffold.⁹ Finally, we systematically incorporated additional substitutions in the B ring of the RABI analogues to determine molecular shape/conformational requirements for their anticancer potency. Biological testing of those RABI compounds revealed their excellent antiproliferative activity against several cancer cell lines including multidrug-resistant cancer cell lines. Mechanism of action of RABIs was investigated using cell cycle analysis, tubulin polymerization assay, competitive mass spectrometry binding assay, and molecular modeling. These studies showed that their antitumor activity was achieved through the antimitotic effect by the inhibition of tubulin polymerization, similar to their parental ABI analogues.

CHEMISTRY

The general synthesis of the A ring modified analogues (**5a–c**) of ABI compounds is outlined in Scheme 1 using the same protocol as the method reported previously.^{3,4,7} The general synthesis of the substituted imidazoles (**8a–e**) follows in Scheme 2. A series of diketones (**7a–e**)¹⁰ in ethanol reacted with 3,4,5-trimethoxy benzeneacetaldehyde **6** and ammonium hydroxide to generate a series of substituted imidazoles.¹¹ RABI

Received: January 18, 2013

Published: April 2, 2013



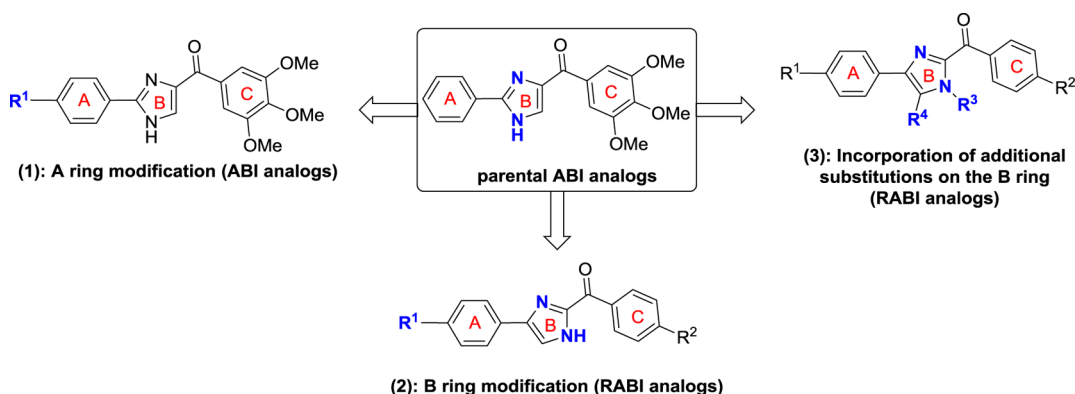
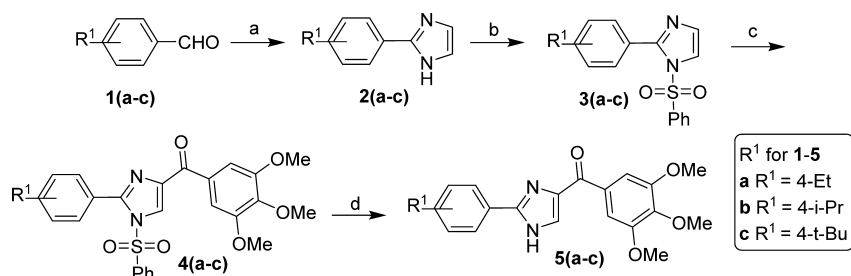


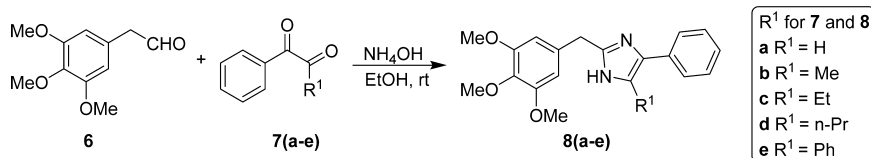
Figure 1. Design protocol for synthesis of RABI analogues.

Scheme 1^a

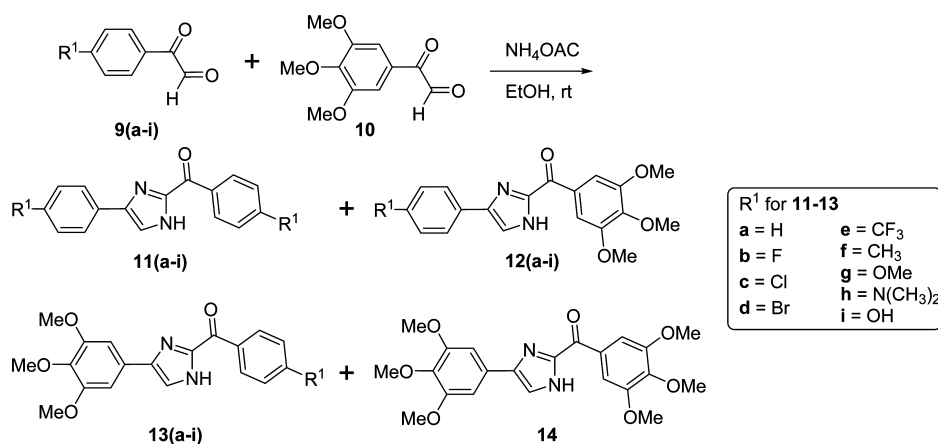


^aReagents and conditions: (a) oxalaldehyde, NH₄OH, EtOH, 0 °C–rt; (b) NaH, PhSO₂Cl, THF, 0 °C–rt; (c) *t*-BuLi, substituted benzoyl chloride, THF, –78 °C; (d) Bu₄NF, THF, rt.

Scheme 2

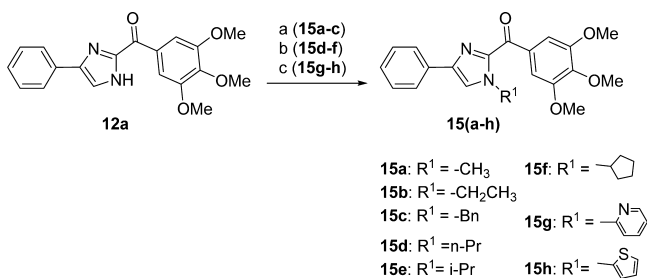


Scheme 3



compounds (11–14) were synthesized utilizing a one-pot, one-step reaction, which is outlined in Scheme 3.⁹ The arylglyoxal¹² reacts with 3,4,5-trimethoxyphenyl glyoxal in the presence of ammonium acetate in ethanol to give four products with similar yields around 20% in one pot. The ratio of compounds 12a–i to 13a–i is approximately 1:1. Two dimensional ¹H–¹³C heteronuclear multiple bond correction spectroscopy (HMBC)

NMR experiments were used to distinguish the structures between 12a–i and 13a–i (Figure S1, Supporting Information). Strategies to incorporate additional substitutions on the B ring of the RABI compounds are shown in Scheme 4. In Scheme 4, there are three conditions to introduce substitution to the N1-position. In condition a, compound 12a react with methyl iodide, ethyl bromide, and benzyl bromide in the

Scheme 4^a

^aReagents and conditions: (a) NaH, CH₃I for **15a**, CH₃CH₂Br for **15b**, and BnBr for **15c**; (b) K₂CO₃, ACN, CH₃CH₂CH₂I for **15d**, (CH₃)₂CHI for **15e**, and cyclopentyl bromide for **15f**; (c) CuI, Cs₂CO₃, DMF, ligand, 2-bromo-pyridine for **15g**, 2-bromothiophene for **15h**.

presence of sodium hydride in anhydrous THF to generate compounds **15a–c**.⁷ In condition b, compound **12a** reacts with *n*-propyl iodide, *i*-propyl iodide, and cyclopentyl bromide in the presence of potassium carbonate in acetonitrile to generate compounds **15d–f**.^{13,14} In condition c, copper iodide, cesium carbonate, and a ligand are used to introduce a pyridine ring or a thiophene ring to N1-position of compound **12a** to make compound **15g–h**.¹⁵ A similar method to that in Scheme 3 was employed to synthesize a series of 5-substituted RABI compounds (**17a–c**), as shown in Scheme 5.

BIOLOGICAL RESULTS AND DISCUSSION

All the compounds were evaluated for their cytotoxicity in human melanoma cell lines and prostate cancer cell lines. Colchicine, vinblastine and docetaxel, the well-known anti-mitotic agents were included in the assays, serving as positive controls and as basis for comparison. The results are summarized in Tables 1–4.

Effect of Substitutions on the A Ring of ABI Analogues. As shown in Table 1, compound **5a** (average IC₅₀ = 18 nM) maintained potent activity in most cancer cells compared with compound **5da**^{3,6} (average IC₅₀ = 10 nM), which has a methyl substitution on the A ring para position. Introducing a larger isopropyl group (**5b**, average IC₅₀ = 254 nM) into this position on the A ring caused a 20-fold decrease of potency compared with compound **5da**. Further increasing the size of this substitution using a *tert*-butyl group to this position resulted in a 100-fold loss of activity compared with **5da**. The activity trend in terms of para substitution in this A ring is Me > Et > H > *i*-Pr > *t*-Bu, clearly suggesting a relatively small binding pocket to the receptor around the A ring, with a methyl group being the optimal size. Because A ring

modification did not generate a more potent compound than **5da**, we decided to design and synthesize analogues by modifying the B ring.

The Ketone Linker Remains Critical for RABI Analogues. We previously reported that a ketone linker is essential for the activity of the parental ABI and its related analogues;¹⁶ to test whether this is still a critical requirement, we synthesized five RABI analogues containing a methylene linker instead of a carbonyl linker (Scheme 2). The biological activity of these five compounds is shown in Table 2. All of them were basically inactive, consistent with results reported previously which indicated the essential role of the carbonyl linker.

Effect of Substitutions on the A Ring of RABIs. After confirming the essential role of the carbonyl linker in the RABI analogues, we converted the methylene linker to carbonyl linker using a slightly modified approach as shown in Scheme 3 and produced RABI analogues **11–13**. All RABI compounds were evaluated for their antiproliferative activity, and the results were shown in Table 3. Compound **12a** was most potent with IC₅₀ values ranging from 6 to 24 nM. Introducing an electron withdrawing group with increasing sizes to the para position on the A ring (4-fluoro, 4-chloro, 4-bromo, and 4-trifluoromethyl) generally decreased activity (compare **12b–e** with **12a**). Among the three halogen substituted RABI compounds, the trend of activity was F < Cl < Br. Introduction of an electron donating group such as methyl to the compound maintained the activity (**12f** IC₅₀, 10–27 nM), while the introduction of methoxy and dimethylamino group caused loss of activity to some extent (**12g** IC₅₀, 30–210 nM; **12h** IC₅₀, 96–263 nM). Compound **12i** with phenol group as A ring was the least potent one among compounds **12a–i**. These results are consistent with the structure–activity relationships identified in the parental ABI analogues (Table 1 and earlier studies^{3,7}).

Effect of Substitutions on the C Ring of RABIs. Several RABI compounds (**11a–i**) which did not have the 3,4,5-trimethoxy moiety on C ring showed poor activity as shown in Table 3. The RABI compounds with unsubstituted phenyl ring as A ring and C ring caused complete loss of activity (**11a** IC₅₀ > 50 μM). Compounds with a single halogen substituent in the para position of A and C rings lost activity completely (IC₅₀ > 5 μM for **11b–d**). When methyl, methoxy, trifluoromethyl, dimethylamino, or hydroxyl was introduced to the para position of the A and C rings, the activity was also lost. All these results suggested the essential role of 3,4,5-trimethoxy substituents on the C ring. Interestingly, when a 3,4,5-trimethoxy group was put on the A ring, the activity of two compounds **13a** and **13d** returned to some extent (**13a** IC₅₀, 195–5770 nM; **13d** IC₅₀, 131–429 nM) even though there is no 3,4,5-trimethoxy substituents on the C ring, perhaps suggesting that the

Scheme 5

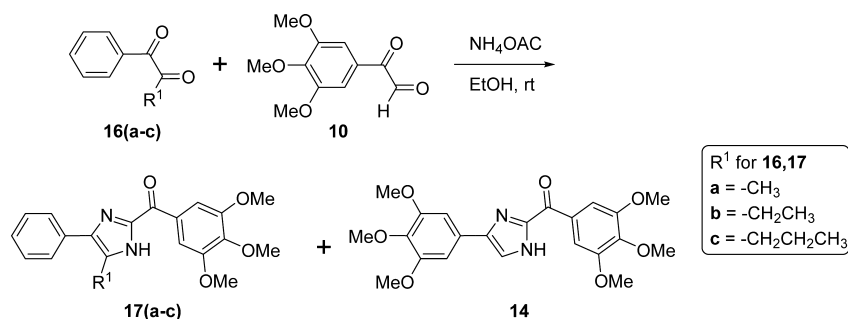


Table 1. In Vitro Growth Inhibitory Effects of ABI Compounds with A Ring Substitution^a

Structure	ID	R ¹	IC ₅₀ ± SEM(nM)							Average IC ₅₀
			LNCaP	PC3	PPC1	DU145	A375	MDA-MB-435	MDA-MB-435/LCC6MDR1	
	5aa ³	H	152 ± 35	288 ± 30	133 ± 6	196 ± 29	160 ± 20	ND	ND	186
	5da ³	Me	12 ± 1	9 ± 0.4	15 ± 1	11 ± 0.1	9 ± 2	5 ± 1	11 ± 2	10
	5a	Et	9 ± 1	13 ± 1	15 ± 1	25 ± 2	14 ± 5	25 ± 4	27 ± 3	18
	5b	i-Pr	171 ± 34	136 ± 20	173 ± 0.3	482 ± 40	ND	312 ± 4	250 ± 4	254
	5c	t-Bu	423 ± 71	436 ± 115	294 ± 2	1698 ± 400	ND	3691 ± 60	3074 ± 50	1603

^aND: not determined.Table 2. In Vitro Growth Inhibitory Effects of RABI Compounds with Methylene Linker^a

Structure	ID	R ¹	IC ₅₀ ± SEM (μM)		
			A375	MDA-MB-435	MDA-MB-435/LCC6MDR1
	8a	H	10.2 ± 0.4	ND	ND
	8b	Me	> 50	ND	ND
	8c	Et	ND	> 50	> 50
	8d	n-Pr	ND	10.9 ± 0.1	15.9 ± 0.2
	8e	Ph	ND	> 50	> 50

^aND: not determined.Table 3. In Vitro Growth Inhibitory Effects of RABI Compounds without B Ring Substitution^a

Structure	ID	R ¹	R ²	IC ₅₀ ± SEM(nM)							
				LNCaP	PC3	PPC1	DU145	A375	WM164	MDA-MB-435	MDA-MB-435/LCC6MDR1
	11a	H	H	> 50000	> 50000	> 50000	> 50000	> 50000	> 50000	> 50000	> 50000
	11b	F	F	> 50000	> 50000	> 50000	> 50000	> 50000	> 50000	> 50000	> 50000
	11c	Cl	Cl	> 50000	> 50000	> 50000	> 50000	35674 ± 665	> 50000	> 50000	> 50000
	11d	Br	Br	16930 ± 6183	18940 ± 1068	13210 ± 706	25490 ± 5144	24960 ± 35	26320 ± 211	14355 ± 178	17814 ± 155
	11e	CF ₃	CF ₃	> 50000	> 50000	> 50000	> 50000	> 50000	> 50000	> 50000	26460 ± 533
	11f	Me	Me	3762 ± 1720	5159 ± 386	2405 ± 308	6541 ± 460	2535 ± 30	3693 ± 18	3020 ± 23	3271 ± 33
	11g	OMe	OMe	6419 ± 4365	23370 ± 1471	38150 ± 2325	9839 ± 503	> 50000	> 50000	> 50000	> 50000
	11h	N(CH ₃) ₂	N(CH ₃) ₂	ND	ND	ND	ND	> 50000	> 50000	> 50000	> 50000
	11i	OH	OH	ND	ND	ND	ND	38769 ± 97	48218 ± 113	47986 ± 104	21421 ± 93
	12a	H	3,4,5-(OMe) ₃	6 ± 1	14 ± 1	13 ± 0.3	22 ± 2	9 ± 6	14 ± 3	24 ± 3	11 ± 2
	12b	F	3,4,5-(OMe) ₃	114 ± 7	196 ± 6	134 ± 0.1	353 ± 10	197 ± 15	298 ± 13	320 ± 14	263 ± 10
	12c	Cl	3,4,5-(OMe) ₃	22 ± 6	64 ± 7	51 ± 1	125 ± 12	51 ± 13	63 ± 11	106 ± 15	75 ± 11
	12d	Br	3,4,5-(OMe) ₃	15 ± 5	33 ± 2	30 ± 1	66 ± 2	29 ± 7	31 ± 4	58 ± 14	43 ± 11
	12e	CF ₃	3,4,5-(OMe) ₃	47 ± 35	93 ± 3	74 ± 2	210 ± 18	123 ± 18	143 ± 8	120 ± 15	175 ± 9
	12f	CH ₃	3,4,5-(OMe) ₃	13 ± 1	19 ± 1	18 ± 0.3	30 ± 4	13 ± 2	14 ± 3	27 ± 11	21 ± 5
	12g	OMe	3,4,5-(OMe) ₃	30 ± 14	61 ± 4	54 ± 1	210 ± 147	33 ± 8	41 ± 12	55 ± 9	59 ± 18
	12h	N(CH ₃) ₂	3,4,5-(OMe) ₃	96 ± 6	118 ± 17	120 ± 12	263 ± 16	141 ± 23	129 ± 19	200 ± 20	162 ± 12
	12i	OH	3,4,5-(OMe) ₃	219 ± 101	155 ± 23	122 ± 6	518 ± 10	487 ± 35	549 ± 24	669 ± 31	455 ± 29
	13a	3,4,5-(OMe) ₃	H	195 ± 91	632 ± 42	408 ± 11	1301 ± 264	1023 ± 23	1273 ± 30	4606 ± 78	5770 ± 63
	13d	3,4,5-(OMe) ₃	Br	131 ± 175	371 ± 247	106 ± 3	429 ± 0.2	136 ± 12	177 ± 16	186 ± 11	161 ± 11
	13g	3,4,5-(OMe) ₃	OMe	708 ± 334	10390 ± 6646	5685 ± 325	> 50000	35414 ± 106	36007 ± 98	10956 ± 96	11428 ± 87
	13h	3,4,5-(OMe) ₃	N(CH ₃) ₂	ND	ND	ND	ND	47878 ± 563	46131 ± 98	29175 ± 88	40618 ± 112
	13i	3,4,5-(OMe) ₃	OH	ND	ND	ND	ND	> 50000	> 50000	> 50000	> 50000
	14	3,4,5-(OMe) ₃	3,4,5-(OMe) ₃	> 50000	> 50000	> 50000	> 50000	> 50000	> 50000	> 50000	> 50000

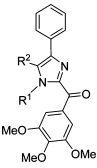
^aND: not determined.

orientation of the compound changed when binding to tubulin. One results worth noting is that when 3,4,5-trimethoxy group was introduced to both the A ring and the C ring, the activity was lost completely. This is consistent with results in previous sections that a bulky A ring containing a 3,4,5-trimethoxy moiety cannot be tolerated at the receptor.

Effect of Substitutions on the B Ring of RABIs. Modifications on the B ring in two different sites were investigated: the N1- and 5-position of the imidazole ring. Introducing methyl, ethyl, or propyl at the 5-position of the imidazole ring resulted in inactive compounds (17a–c) as shown in Table 4. A trend in activity for the substituted alkyl groups, Me > Et > Pr, was also observed, which suggests big

bulky groups at this position are detrimental to activity. In contrast, when different substitution groups were introduced to the N1-position of the imidazole ring, the activity was maintained with only minimal loss compared with the parent compound, 12a. First, some alkyl groups were tried on the N1-position including methyl, ethyl, *n*-propyl, *i*-propyl, and cyclopentyl groups. Introduction of methyl did not affect the activity compared with 12a (15a IC₅₀ 9–26 nM), while the activity began to lose as the size of the alkyl groups increased, suggesting that a bulky alkyl group at this position was unfavorable. Benzyl group, which was also a relatively big group at the N1-position of the imidazole ring, decreased the activity (15c IC₅₀ 34–160 nM). Surprisingly, when the substituents

Table 4. In Vitro Growth Inhibitory Effects of RABI Compounds with B Ring Substitution^a

Structure	ID	R ¹	R ²	IC ₅₀ ± SEM (nM)							
				LNCaP	PC3	PPC1	DU145	A375	WM164	MDA-MB-435	MDA-MB-435/LCC6MDR1
	15a	Me	H	10 ± 1	16 ± 1	13 ± 0.2	26 ± 3	9 ± 2	33 ± 5	16 ± 2	18 ± 2
	15b	Et	H	29 ± 20	25 ± 4	30 ± 8	66 ± 2	28 ± 3	16 ± 3	26 ± 3	33 ± 4
	15c	Bn	H	66 ± 6	72 ± 5	77 ± 2	160 ± 41	104 ± 17	34 ± 7	94 ± 18	156 ± 18
	15d	n-Pr	H	49 ± 10	26 ± 6	10 ± 4	72 ± 13	42 ± 3	14 ± 3	37 ± 2	44 ± 4
	15e	i-Pr	H	62 ± 8	53 ± 9	15 ± 3	114 ± 20	38 ± 4	23 ± 5	18 ± 3	44 ± 4
	15f		H	51 ± 6	56 ± 1	63 ± 4	167 ± 16	135 ± 13	56 ± 13	134 ± 15	161 ± 19
	15g		H	20 ± 5	11 ± 3	8 ± 2	37 ± 6	14 ± 3	6 ± 1	11 ± 3	15 ± 5
	15h		H	ND	ND	ND	ND	20 ± 2	8 ± 2	25 ± 3	27 ± 3
	17a	H	Me	938 ± 65	1617 ± 144	860 ± 5	2001 ± 163	1302 ± 106	1897 ± 116	1634 ± 102	1586 ± 104
	17b	H	Et	2029 ± 880	3654 ± 192	2078 ± 90	5079 ± 635	2151 ± 48	5514 ± 35	8795 ± 23	5114 ± 27
	17c	H	n-Pr	3094 ± 330	12360 ± 7566	11410 ± 5918	16350 ± 6724	36977 ± 73	19595 ± 91	30540 ± 103	14270 ± 362

^aND: not determined.

were changed from alkyl groups to heterocyclic rings, the “effect of big size” disappeared. The introduction of a pyridine ring to the N1-position generated a very potent compound, with IC₅₀ ranging from 6 to 37 nM. The introduction of a thiophene ring also produced a potent compound, with IC₅₀ ranging from 8 to 20 nM. The excellent activity of **15g** and **15h** promises the future optimization at this position using other ring systems.

Effect of RABI Compounds against Multidrug-Resistant Melanoma Cells. Pgp-mediated drug efflux represents a major mechanism for cancer cells to prevent the buildup of effective intracellular drug concentrations. We have previously shown that the parent ABI analogues can effectively overcome a variety of clinically relevant multidrug resistant mechanisms including Pgp-mediated drug resistance.^{5,6} To determine whether the new RABI analogues maintain this ability, we compared the activity of the RABI compounds against multidrug-resistant melanoma cells (MDA-MB-435/LCCMDR1) and their parental nonresistant cancer cells (MDA-MB-435). This pair of cell lines have been well validated and widely used to assess abilities of drugs overcoming Pgp-mediated MDR.^{17–20} Compound **12a**, **12d**, and **12e**, together with colchicine, vinblastine, and paclitaxel, were tested on both the MDR melanoma cells and their parental melanoma cell lines (Table 5). Compounds **12a**, **12d**, and **12e** showed much

even better activity against Pgp-overexpressed melanoma cells than their parental, nonresistant melanoma cells.

Mechanism of Action Studies on RABIs. Because the parental ABI analogues kills cancer cells by inhibiting mitotic process, we hypothesized that RABIs maintain their mechanism of action. To test this hypothesis, we first performed the cell cycle analysis after the treatment of RABIs on PC3 cells. Cell cycle distribution was determined by propidium iodide (PI) staining. Treated cells were fixed with 70% ice-cold ethanol, and the fixed cells were stained with PI in the presence of RNase A. Cell cycle distribution was analyzed by fluorescence-activated cell sorting (FACS) analysis. Compound **5a**, **12a**, **12d**, **12f**, **15a**, and **15b** were treated on PC3 cells for 24 h. Four different concentrations, 1, 10, 50, and 100 nM, of each compound were chosen to examine the dose effect. Results indicated that RABIs arrest cells in the G₂/M phase (Figure. 2A). In the vehicle treated group, about 18% of PC3 cells were distributed in the G₂/M phase. RABIs increased the proportion of cells in G₂/M phase up to 70% approximately in a concentration-dependent manner (Figure. 2B). The potency of the different concentrations in arresting cells in the G₂/M phase positively correlated with in vitro cell growth inhibitory activity.

On the basis of their effect on cell cycle distribution, we next investigated the effect on tubulin polymerization of RABI analogues. To determine the effect of drug on tubulin polymerization, a fluorescence-enhanced tubulin polymerization assay kit was used. The control drug, vinblastine, inhibited tubulin polymerization and destabilized microtubule, while paclitaxel promoted microtubule stability (Figure S2, Supporting Information). RABI compounds **12a** and **15a** inhibited tubulin polymerization as the tubulin destabilizer, vinblastine in a concentration-dependent manner (Figure S2, Supporting Information), and **15a** showed more potent inhibitory effect than **12a**. In the competitive mass spectrometry binding assay, the amount of unbound colchicine in the presence or absence of any competitor would explain whether there is the competition of compounds and colchicine to bind in tubulin. **12a** and **15g** competed effectively with colchicine for tubulin binding (Figure S3, Supporting Information) with potency similar to podophyllotoxin. Vinblastine, the negative control, did not inhibit colchicine binding to tubulin. Collectively, these data confirmed that new RABI analogues maintain their antimitotic mechanisms of action, most likely binding to the colchicine binding site in tubulin, as is the case for the parental ABI analogues.^{6,7}

Molecular Modeling Studies. One surprising results from the analysis of the structure–activity relationships for the RABI

Table 5. In Vitro Growth Inhibitory Effects of RABI Compounds Comparison to Other Anticancer Drugs on Multidrug-Resistant Melanoma Cells and Parent Cell Line

compd	IC ₅₀ ± SEM (nM)		
	MDA-MB-435	MDA-MB-435/LCC6MDR1	resistance index
12a	24 ± 3	11 ± 2	0.5
12d	58 ± 14	43 ± 11	0.7
12e	27 ± 11	21 ± 5	0.8
colchicine	11 ± 2	643 ± 9	58.5
vinblastine	0.4 ± 0.1	11 ± 1	27.5
paclitaxel	4 ± 1	277 ± 41	69.3

better resistance index (0.5 for **12a**, 0.7 for **12d**, 0.8 for **12e**) than colchicine (58.5), vinblastine (27.5), and paclitaxel (69.3). Although colchicine, vinblastine, and paclitaxel showed excellent activity in nonresistant melanoma cell lines, they were much less potent in resistant melanoma cell lines. In contrast, compounds **12a**, **12d**, and **12e** showed comparable or

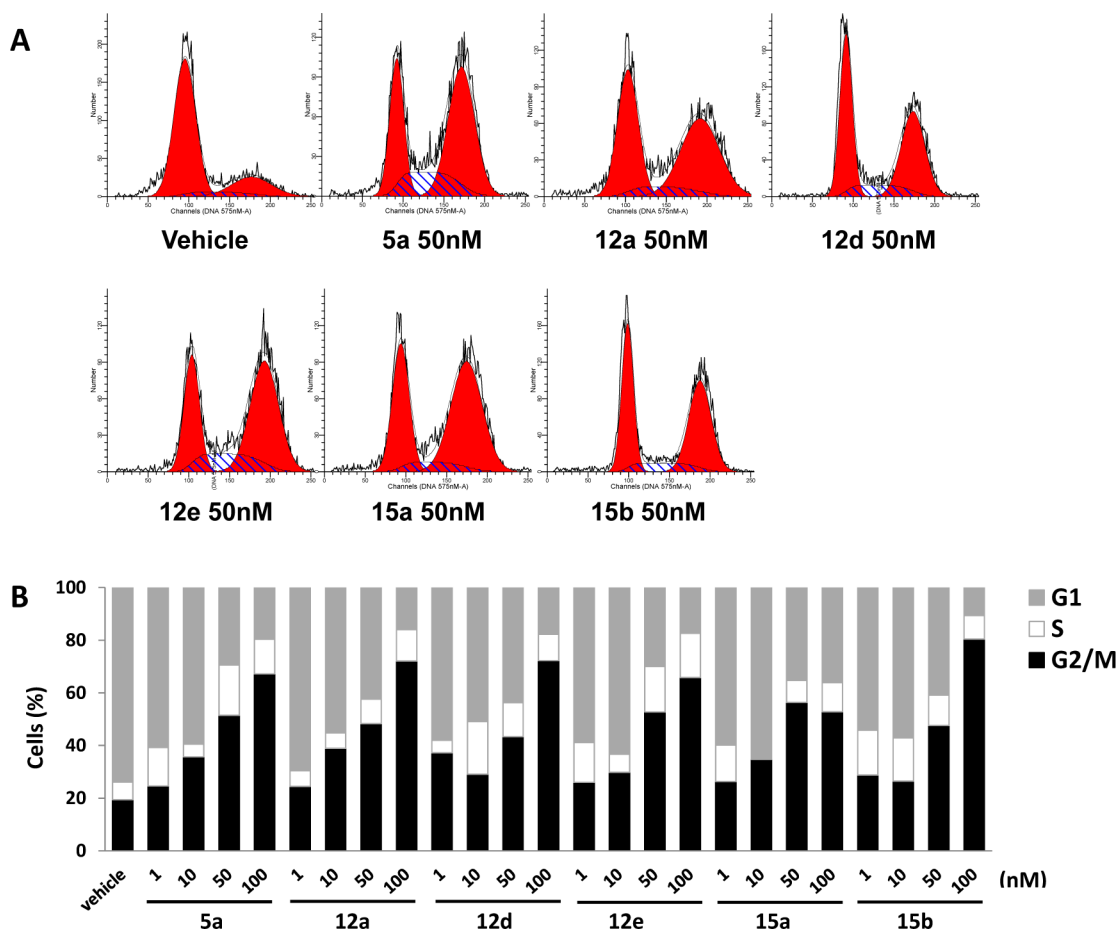


Figure 2. Effect of compounds 5a, 12a, 12d, 12e, 15a, and 15b on cell cycle.

analogues is that incorporating a 5- or 6-membered heterocyclic ring substitution at the N1-position in the B ring produced highly active compounds, while both similar-sized alkyl substitutions or a larger benzyl substitution resulted in significantly reduced activity (Table 4). To better understand how the N1-substituted RABI analogues interact with tubulin, the potential binding modes for two of the most potent compounds, 12a and 15g, were investigated at the colchicine binding site in tubulin dimer using the Schrodinger 2011 molecular modeling suite (Schrodinger, Inc., New York, NY). Both compounds were docked into two different tubulin crystal structure (PDB ID code: 1SA0 or 3HKD), representing two potential binding geometries for colchicine site ligands. Interestingly, nonsubstituted RABI analogue 12a demonstrated best Glide docking score of -9.2 in 3HKD compared with a score of -6.4 in 1SA0, while substituted RABI analogue 15g showed best Glide score of -9.0 in 1SA0 and could not fit into the binding pocket of 3HKD.

The overview of the binding site of 12a and TN-16 (native ligand of 3HKD) is shown in Figure 3A. This binding pocket is located on the interface between the α - and β -subunits of the tubulin dimer and extended slightly out of the β -subunit.^{21,22} Figure 3B illustrated the close view of the potential binding pose. Generally, 12a (green stick) overlapped well with TN-16 (blue stick). The A ring of 12a went deep into the pocket and overlapped very well with the first phenyl ring of TN-16. There is very little space between the A ring and its surrounding amino acids in the β -subunit (Figure 3B), and this explains why little tolerance is allowed for larger substitution in the A ring for

both ABI and RABI compounds. The imidazole ring overlapped well with the pyrrolidinedione ring of TN-16. A potential hydrogen bond is formed between the imidazole NH of 12a and VAL238 in β -H7 (Figure 3B), similar to the one formed between the native ligand TN-16 and VAL238 in β -H7. This hydrogen bond stabilized the interaction of 12a with the binding pocket. The 3,4,5-trimethoxybenzoyl group (C ring) of 12a extends toward the α/β -tubulin interface, similar to the mode of the active parental ABI analogues.^{4,7}

Unlike 12a, which does not possess a large N1-substitution, the much "fatter" RABI 15g cannot fit into the cylinder shaped binding pocket in 3HKD but docks reasonably well into the shallower pocket in 1SA0. The potential binding mode of 15g is shown in Figure 3C,D. Figure 3C shows the general view of the binding site of 15g and the native ligand colchicine in 1SA0. Figure 3D illustrates the closed view of the potential binding pose. Interestingly, in this binding mode, part of 15g (green stick) overlapped well with the native ligand colchicine (blue stick), while the original A ring of 15g extended out of the colchicine binding pocket into the α/β -tubulin interface. The pyridine ring substitute on the N1- position occupied the site where the 7-membered ring in colchicine binds, while the 3,4,5-trimethoxybenzoyl group (C ring) of 15g overlapped very well with the 3,4,5-trimethoxyphenyl ring in colchicine. A hydrogen bond between the oxygen of 4-OMe in 15g and SH group of β -CYS241 stabilized the interaction. A similar hydrogen bond was also observed between the oxygen of one methoxy group in colchicine and SH of β -CYS241. This binding mode is well consistent with the structure–activity relationships observed for

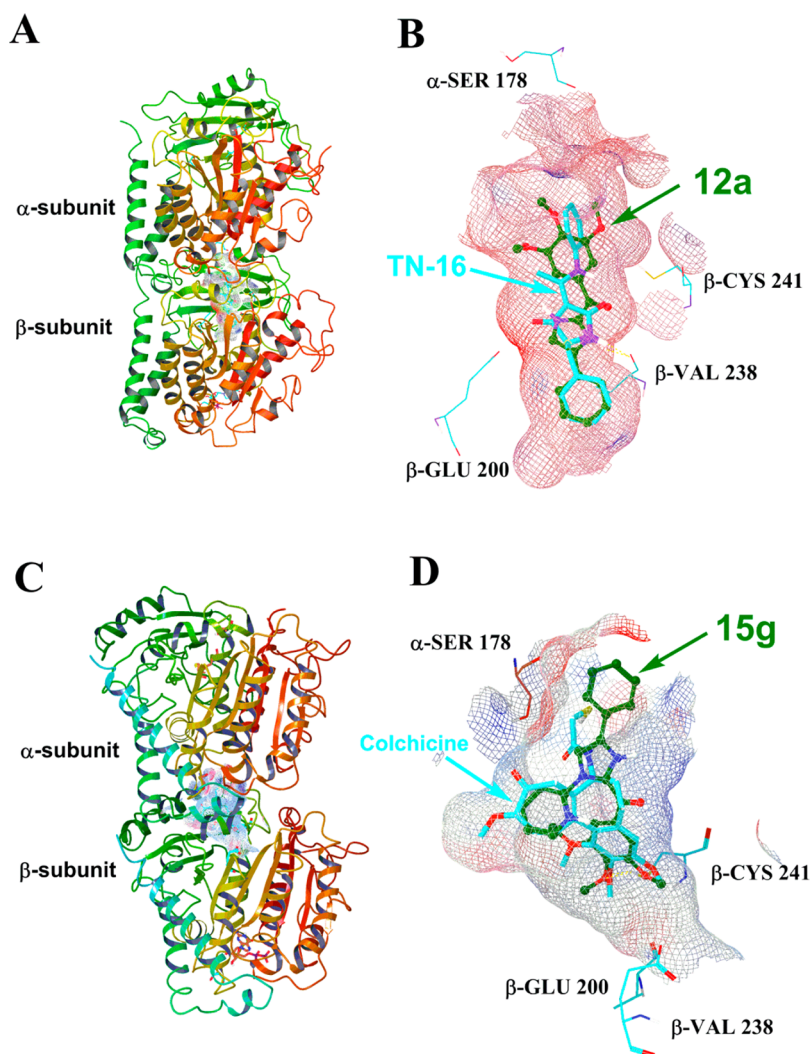


Figure 3. (A) The overview of the binding modes of **12a** and the native ligand TN-16 in tubulin crystal structure 3HKD. (B) The close view of the potential binding pose of **12a** and TN-16 in 3HKD. (C) The overview of the binding modes of **15g** and the native ligand colchicine in tubulin crystal structure 1SA0. (D) The close view of the potential binding pose of **15g** and colchicine in 1SA0.

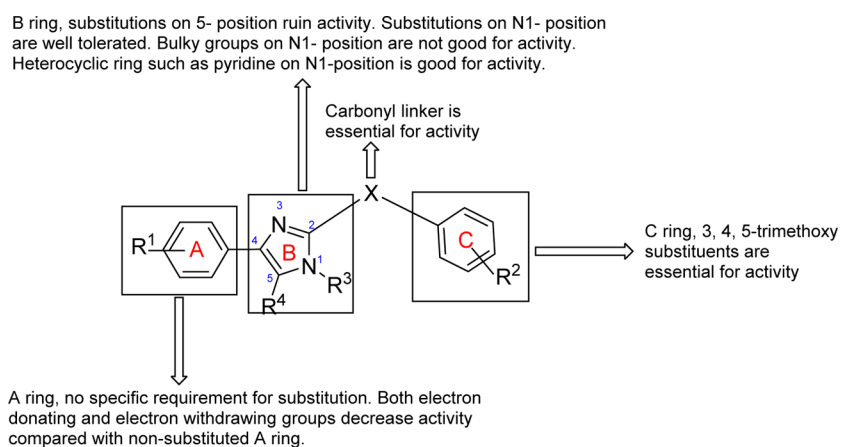


Figure 4. SAR of RABI analogues.

substituted RABI compounds: a smaller, alkyl substitution could not fill this region of the binding pocket and lacks the planar geometry required for binding, while too large a benzyl substitution could not fit into the pocket and also lacks the needed geometry. A 5- or 6-membered heterocyclic ring has the

desirable shape and size to fit into the pocket well. These data also suggest that while the original “A ring” may not be critical for binding when a suitable N1-substitution is present, an optimized substitution replacing this original A ring moiety may take advantage of the added interactions between the ligand

and receptor and provide even better ligand than **15g**. Work toward this direction is current ongoing and will be reported in the future.

CONCLUSIONS

In summary, novel RABI analogues were designed and synthesized based on rational structural modification of previous ABI analogues. Structure–activity relationships (Figure 4) were investigated by introducing different substituents into the A, B, and C rings. Several RABIs showed excellent antiproliferative activity which was comparable to existing tubulin-targeting agents such as paclitaxel, colchicine, or vinblastine but could overcome Pgp-mediated multiple drug resistance effectively. Among them compound **12a** was the most potent one, with IC_{50} in the low nanomolar range, while compound **15g** provided very interesting insights in future optimization of these analogues. Mechanism of action studies confirmed that RABI analogues maintain their ability to inhibit tubulin polymerization at colchicine binding site and arresting cells in G_2/M phase. These results strongly suggest that novel RABI analogues can be further developed as a promising antitumor agent for the more efficacious treatment of advanced cancers.

EXPERIMENTAL SECTION

General. All reagents were purchased from Sigma-Aldrich Chemical Co., Fisher Scientific (Pittsburgh, PA), Alfa Aesar (Ward Hill, MA), and AK Scientific (Mountain View, CA) and were used without further purification. Routine thin layer chromatography (TLC) was performed on aluminum-backed Uniplates (Analtech, Newark, DE). NMR spectra were obtained on a Varian Inova-500 spectrometer (Agilent Technologies, Santa Clara, CA) or a Bruker Ascend 400 (Billerica, MA) spectrometer. Chemical shifts are reported as parts per million (ppm) relative to TMS in $CDCl_3$. High resolution mass spectra were collected on a Waters Xevo G2-S ToF instrument. The purity of the final compounds was tested via Agilent series HPLC system (Agilent 1100 Series, Agilent 1100 Chemstation, Agilent Technology Co, Ltd.) installed with a photodiode array detector. Four RP-HPLC methods were conducted using a Phenomenex $5 \mu m$ C-18 column (250 mm \times 4.6 mm) at ambient temperature and a flow rate of 1.0 mL/min. HPLC1: solvent A (water) and solvent B (methanol), 0–30 min 90% B. HPLC2: solvent A (water) and solvent B (methanol), 0–30 min 85%. HPLC3: solvent A (water) and solvent B (methanol), 0–30 min 80% B. HPLC4: solvent A (water) and solvent B (methanol), 0–15 min 50–100% B (linear gradient), 15–25 min 100% B, 25–28 min 100–50% B, 28–33 min 50% B. UV detection at 254 nm. Purities of the compounds were established by careful integration of areas for all peaks detected and are reported for each compound in the following section.

General Procedure for the Preparation of 2-Aryl-1H-imidazole (2a–c). To a solution of appropriate benzaldehyde **1** (100 mmol) in ethanol (350 mL) at 0 °C was added a solution of 40% oxalaldehyde in water (12.8 mL, 110 mmol) and a solution of 29% ammonium hydroxide in water (1000 mmol, 140 mL). After stirring for 2–3 days at room temperature, the reaction mixture was concentrated and the residue was subjected to flash column chromatography with dichloromethane as eluent to yield the titled compound as a yellow powder. Yield: 20–40%.

General Procedure for the Preparation of 2-Aryl-1-(phenylsulfonyl)-1H-imidazole (3a–c). To a solution of 2-aryl-1H-imidazole **2** (20 mmol) in anhydrous THF (200 mL) at 0 °C was added sodium hydride (60% dispersion in mineral oil, 1.2 g, 30 mmol) and stirred for 30 min. Benzenesulfonyl chloride (2.82 mL, 22 mmol) was added, and the reaction mixture was stirred overnight. After dilution by 100 mL of saturated $NaHCO_3$ solution (aqueous), the reaction mixture was extracted by ethyl acetate (500 mL). The organic layer was dried over magnesium sulfate and concentrated. The residue was purified by flash

column chromatography (hexane:ethyl acetate 2:1) to give a pale solid. Yield: 40–50%.

General Procedure for the Preparation of Aryl (2-Aryl-1-(phenylsulfonyl)-1H-imidazol-4-yl)methanone (4a–c). To a solution of 2-aryl-1-(phenylsulfonyl)-1H-imidazole (6.0 mmol) **3** in anhydrous THF (30 mL) at –78 °C was added 1.7 M *tert*-butyl lithium in pentane (5.3 mL, 9.0 mmol) and stirred for 10 min. Appropriate substituted benzoyl chloride (7.2 mmol) was added at –78 °C and stirred for overnight. The reaction mixture was diluted with 100 mL of saturated $NaHCO_3$ solution (aqueous) and extracted by ethyl acetate (200 mL). The organic layer was dried over magnesium sulfate and concentrated. The residue was purified by flash column chromatography (hexane:ethyl acetate 4:1) to give a white solid. (Note: Due to the limited amount of starting material or the difficulty of separation, the following products formed in this step were used without further purification as a mixture for the next step.) Yield: 15–40%.

General Procedure for the Preparation of Aryl (2-Aryl-1H-imidazol-4-yl)methanone (5a–c). To a solution of aryl (2-aryl-1-(phenylsulfonyl)-1H-imidazol-4-yl) methanone (2.0 mmol) **4** in THF (20.0 mL) was added 1.0 M tetrabutyl ammoniumfluoride (4.0 mmol) and stirred overnight. The reaction mixture was diluted by 50 mL of saturated $NaHCO_3$ solution (aqueous) and extracted by ethyl acetate (100 mL). The organic layer was dried over magnesium sulfate and concentrated. The residue was purified by flash column chromatography (hexane:ethyl acetate 3:1) or recrystallized from water and methanol to give a white solid. Yield: 80–95%.

(2-(4-Ethylphenyl)-1H-imidazol-4-yl)(3,4,5-trimethoxyphenyl)methanone (5a). 1H NMR (500 MHz, $CDCl_3$) δ 10.40 (br, 1H), 7.92 (d, J = 8.0 Hz, 2H), 7.85 (s, 1H), 7.36 (d, J = 8.0 Hz, 2H), 7.27 (s, 2H), 3.99 (s, 3H), 3.97 (s, 6H), 2.75 (q, d = 7.5 Hz, 2H), 1.313 (t, d = 7.5 Hz, 3H). Exact mass for $C_{21}H_{22}N_2O_4$: 366.158. HRMS: $[M + H]^+$: 367.1764. HPLC1: t_R 4.97 min, purity 97.8%.

(2-(4-Isopropylphenyl)-1H-imidazol-4-yl)(3,4,5-trimethoxyphenyl)methanone (5b). 1H NMR (500 MHz, $CDCl_3$) δ 10.38 (br, 1H), 7.82 (d, J = 8.0 Hz, 2H), 7.75 (s, 1H), 7.38 (d, J = 8.0 Hz, 2H), 7.15 (s, 2 H), 3.88 (s, 3H), 3.86 (s, 6H), 2.90 (m, 1H), 1.331(d, d = 6.5 Hz, 6H); Exact Mass for $C_{22}H_{24}N_2O_4$: 380.1700; HRMS: $[M + H]^+$: 381.1818; HPLC1: t_R 5.26 min, purity 97.5%.

(2-(4-*tert*-Butylphenyl)-1H-imidazol-4-yl)(3,4,5-trimethoxyphenyl)methanone (5c). 1H NMR (500 MHz, $CDCl_3$) δ 10.42 (br, 1 H), 7.94 (d, J = 8.0 Hz, 2H), 7.84 (s, 1H), 7.54 (d, J = 8.0 Hz, 2H), 7.25 (s, 2H), 3.98 (s, 3H), 3.96 (s, 6H), 1.385(s, 9H). Exact Mass for $C_{23}H_{26}N_2O_4$: 394.1900. HRMS: $[M + H]^+$: 395.2054. HPLC2: t_R 7.75 min, purity >99%.

General Procedure for the Synthesis of 5-(Alkyl or Aryl)-4-phenyl-2-(3,4,5-trimethoxybenzyl)-1H-imidazole and 4-(Alkyl or Aryl)-5-phenyl-2-(3,4,5-trimethoxybenzyl)-1H-imidazole (8a–e). To a solution of the aldehyde **6** (5 mmol) in ethanol (20 mL) at 0 °C was added the phenyl alkyl dione **7** (5.5 mmol) and a solution of 29% ammonium hydroxide in water (50 mmol, 7 mL). After stirring for 2–3 days at room temperature, the reaction mixture was concentrated and the residue was subjected to flash column chromatography with dichloromethane as eluent to yield the titled compound as a yellow powder. Yield: 20–30%.

5-Phenyl-2-(3,4,5-trimethoxybenzyl)-1H-imidazole and 4-Phenyl-2-(3,4,5-trimethoxybenzyl)-1H-imidazole (8a). 1H NMR (500 MHz, chloroform- d) δ 7.91–7.62 (m, 2H), 7.43–7.34 (m, 2H), 7.27–7.21 (m, 2H), 6.51 (s, 2H), 4.12 (s, 2H), 3.86 (s, 3H), 3.84 (s, 6H). Exact mass for $C_{19}H_{20}N_2O_3$: 324.1500. HRMS: $[M + H]^+$: 325.1684.

5-Methyl-4-phenyl-2-(3,4,5-trimethoxybenzyl)-1H-imidazole and 4-Methyl-5-phenyl-2-(3,4,5-trimethoxybenzyl)-1H-imidazole (8b). 1H NMR (500 MHz, chloroform- d) δ 7.55 (d, J = 7.6 Hz, 2H), 7.43–7.37 (m, 2H), 7.25 (d, J = 6.7 Hz, 1H), 6.49 (s, 2H), 4.03 (s, 2H), 3.84 (d, J = 1.3 Hz, 3H), 3.81 (d, J = 1.2 Hz, 6H), 2.42 (s, 3H). Exact mass for $C_{20}H_{22}N_2O_3$: 338.1600. HRMS: $[M + H]^+$: 339.1799.

5-Ethyl-4-phenyl-2-(3,4,5-trimethoxybenzyl)-1H-imidazole and 4-Ethyl-5-phenyl-2-(3,4,5-trimethoxybenzyl)-1H-imidazole (8c). 1H NMR (500 MHz, chloroform- d) δ 8.47 (s, 0.42H), 8.39 (s, 0.58H), 7.86–7.62 (m, 2H), 7.41 (m, 2H), 7.35–7.31 (m, 1H), 6.54 (m, 2H), 4.10 (m, 2H), 3.90–3.83 (m, 9H), 2.79 (m, 2H), 1.38–1.17 (m, 3H). Exact mass for $C_{21}H_{24}N_2O_3$: 352.1800. HRMS: $[M + H]^+$: 353.1912.

4-Phenyl-5-propyl-2-(3,4,5-trimethoxybenzyl)-1H-imidazole and 5-Phenyl-4-propyl-2-(3,4,5-trimethoxybenzyl)-1H-imidazole (8d). ^1H NMR (400 MHz, chloroform- d) δ 8.63 (s, 0.48H), 8.50 (s, 0.52H), 7.70–7.64 (m, 1H), 7.41 (m, 3H), 7.37–7.32 (m, 1H), 6.52 (d, J = 1.3 Hz, 2H), 4.08 (d, J = 5.1 Hz, 2H), 3.87 (m, 3H), 3.86–3.84 (m, 6H), 2.73 (m, 2H), 1.88–1.75 (m, 1H), 1.64 (m, 1H), 0.98 (m, 3H). Exact mass for $\text{C}_{22}\text{H}_{26}\text{N}_2\text{O}_3$: 366.1900. HRMS: $[\text{M} + \text{H}]^+$: 367.2011.

4,5-Diphenyl-2-(3,4,5-trimethoxybenzyl)-1H-imidazole (8e). ^1H NMR (400 MHz, chloroform- d) δ 7.44–7.36 (m, 4H), 7.28–7.20 (m, 6H), 6.50 (s, 2H), 4.08 (s, 2H), 3.78 (m, 9H). Exact mass for $\text{C}_{25}\text{H}_{24}\text{N}_2\text{O}_3$: 400.1800. HRMS: $[\text{M} + \text{H}]^+$: 401.1977.

General Procedure for the Preparation of (4 or 5)-Aryl-2-aryloyl-(1H)-imidazole derivatives (11–14). To ammonium acetate (10 mmol) in ethanol (5 mL) and water (0.3 mL) was added arylglyoxal hydrate **9** (1 mmol) in ethanol (5 mL) and 3,4,5-trimethoxyphenyl glyoxal hydrate **10** (1 mmol) in ethanol (10 mL). The mixture was stirred at room temperature for 30–45 min. The reaction was stopped after the consumption of the starting material monitored by TLC. The mixture was then extracted with ethyl acetate. The organic layer was washed with brine, dried over anhydrous sodium sulfate, and concentrated to get the crude product. The crude was purified by flash chromatography (dichloromethane:methanol 50:1).

Phenyl-(4-phenyl-1H-imidazol-2-yl)methanone and phenyl-(5-phenyl-1H-imidazol-2-yl)methanone (11a). ^1H NMR (500 MHz, DMSO- d_6): δ 13.80 (s, 0.25H), 13.63 (s, 1H), 8.60 (d, J = 7.76 Hz, 2H), 8.47 (d, J = 7.7 Hz, 0.5H), 8.08 (s, 1H), 7.97 (d, J = 7.95 Hz, 0.5H), 7.94 (d, J = 7.64 Hz, 2H), 7.79 (s, 0.25H), 7.69 (t, J = 7.1 Hz, 1H), 7.66 (t, J = 7.6 Hz, 0.25H), 7.60 (t, J = 7.6 Hz, 2H), 7.57 (t, J = 8.1 Hz, 0.5H), 7.47 (t, J = 7.55 Hz, 0.5H), 7.42 (t, J = 7.7 Hz, 2H), 7.37 (t, J = 7.1 Hz, 0.25H), 7.28 (t, J = 7.3 Hz, 1H). Exact mass for $\text{C}_{16}\text{H}_{12}\text{N}_2\text{O}$: 248.095. HRMS: $[\text{M} + \text{H}]^+$: 249.1058. HPLC4: t_R 10.83 min, purity 97.6%.

(4-Fluorophenyl)-(4-(4-fluorophenyl)-1H-imidazol-2-yl)-methanone and (4-Fluorophenyl)-(5-(4-fluorophenyl)-1H-imidazol-2-yl)methanone (11b). ^1H NMR (400 MHz, chloroform- d) δ 10.68 (s, 1H), 10.52 (s, 1H), 8.93–8.82 (dd, J = 5.89, 8.64 Hz, 2H), 8.72 (dd, J = 5.60, 8.70 Hz, 0.39H), 7.89 (dd, J = 5.39, 8.72 Hz, 2H), 7.63 (dd, J = 5.05, 8.25 Hz, 0.46H), 7.59 (d, J = 2.2 Hz, 0.29 H), 7.55 (d, J = 2.8 Hz, 1H), 7.25–7.20 (m, 2H), 7.20–7.13 (m, 2H). Exact mass for $\text{C}_{16}\text{H}_{10}\text{F}_2\text{N}_2\text{O}$: 284.0761. HRMS: $[\text{M} + \text{H}]^+$: 285.0830. HPLC4: t_R 13.97 min, purity 98.0%.

(4-Chlorophenyl)-(4-(4-chlorophenyl)-1H-imidazol-2-yl)-methanone and (4-Chlorophenyl)-(5-(4-chlorophenyl)-1H-imidazol-2-yl)methanone (11c). ^1H NMR (400 MHz, chloroform- d) δ 10.70 (s, 0.65 H), 10.55 (s, 1H), 8.78 (d, J = 8.65 Hz, 2H), 8.63 (s, 1H), 7.87 (s, 2H), 7.66–7.52 (m, 5H), 7.50–7.39 (m, 2H). Exact mass for $\text{C}_{16}\text{H}_{10}\text{Cl}_2\text{N}_2\text{O}$: 316.017. HRMS: $[\text{M} + \text{H}]^+$: 317.0292. HPLC4: t_R 16.30 min, purity 98.8%.

4-Bromophenyl-(4-(4-bromophenyl)-1H-imidazol-2-yl)ketone and 4-Bromophenyl-(5-(4-bromophenyl)-1H-imidazol-2-yl)-methanone (11d). ^1H NMR (500 MHz, DMSO- d_6) δ 13.91 (s, 0.16H), 13.73 (s, 1H), 8.51 (d, J = 8.4 Hz, 2H), 8.42 (d, J = 8.3 Hz, 0.32H), 8.16 (s, 1H), 7.93 (d, J = 8.15 Hz, 0.32H), 7.89 (d, J = 8.35 Hz, 2H), 7.83 (d, J = 8.45 Hz, 2H), 7.80 (d, J = 8.4 Hz, 0.32H), 7.79 (s, 0.16H), 7.67 (d, J = 8.05 Hz, 0.32H), 7.62 (d, J = 8.35 Hz, 2H). Exact mass for $\text{C}_{16}\text{H}_{10}\text{Br}_2\text{N}_2\text{O}$: 403.916. HRMS: $[\text{M} + \text{H}]^+$: 404.9241. HPLC4: t_R 16.53 min, purity 95.5%.

(4-(Trifluoromethyl)phenyl)-(4-(4-(trifluoromethyl)phenyl)-1H-imidazol-2-yl)methanone and (4-(Trifluoromethyl)phenyl)-(5-(4-(trifluoromethyl)phenyl)-1H-imidazol-2-yl)methanone (11e). ^1H NMR (400 MHz, chloroform- d) δ 10.83 (s, 0.38H), 10.60 (s, 1H), 8.78 (d, J = 8.19 Hz, 2H), 8.64 (d, J = 8.13 Hz, 0.48H), 7.93 (d, J = 8.34 Hz, 2H), 7.76 (d, J = 8.56 Hz, 2H), 7.66–7.59 (m, 3H). Exact mass for $\text{C}_{18}\text{H}_{10}\text{F}_6\text{N}_2\text{O}$: 384.0697. HRMS: $[\text{M} + \text{H}]^+$: 385.0790. HPLC1: t_R 7.76 min, purity 98.3%.

p-Tolyl-(4-p-tolyl-1H-imidazol-2-yl)methanone and p-Tolyl-(5-p-tolyl-1H-imidazol-2-yl)methanone (11f). ^1H NMR (400 MHz, chloroform- d) δ 10.96 (s, 1H), 10.73 (s, 1H), 8.71 (d, J = 8.26 Hz, 2H), 8.54 (d, J = 8.23 Hz, 2H), 7.82 (d, J = 8.11 Hz, 2H), 7.67–7.49 (m, 4H), 7.37 (t, J = 7.62, 7.62 Hz, 4H), 7.30 (s, 1H), 7.28 (s, 2H),

7.26 (s, 1H), 2.49 (d, J = 4.52 Hz, 6H), 2.42 (d, J = 4.95 Hz, 6H). Exact mass for $\text{C}_{18}\text{H}_{16}\text{N}_2\text{O}$: 276.1263. HRMS: $[\text{M} + \text{H}]^+$: 277.1385. HPLC3: t_R 10.27 min, purity 98.7%.

(4-Methoxyphenyl)-(4-(4-methoxyphenyl)-1H-imidazol-2-yl)-methanone and (4-Methoxyphenyl)-(5-(4-methoxyphenyl)-1H-imidazol-2-yl)methanone (11g). ^1H NMR (400 MHz, chloroform- d) δ 10.50 (s, 1H), 10.38 (s, 1H), 8.77 (d, J = 8.90 Hz, 2H), 8.60 (d, J = 8.89 Hz, 2H), 7.77 (s, 1H), 7.75 (s, 1H), 7.48 (d, J = 8.75 Hz, 1H), 7.45–7.36 (m, 2H), 7.03–6.87 (m, 5H), 3.86 (s, 2H), 3.85 (s, 2H), 3.84 (s, 2H), 3.80 (s, 2H), 3.79 (s, 2H). Exact mass for $\text{C}_{18}\text{H}_{10}\text{F}_6\text{N}_2\text{O}$: 384.0697. HRMS: $[\text{M} + \text{H}]^+$: 385.0790. HPLC2: t_R 6.05 min, purity 97.2%.

(4-(Dimethylamino)phenyl)-(4-(4-(dimethylamino)phenyl)-1H-imidazol-2-yl)methanone and (4-(Dimethylamino)phenyl)-(5-(4-(dimethylamino)phenyl)-1H-imidazol-2-yl)methanone (11h). ^1H NMR (500 MHz, DMSO- d_6) δ 13.17 (s, 0.35H), 13.12 (s, 1H), 8.64 (d, J = 8.95 Hz, 2H), 8.50 (d, J = 8.95 Hz, 1H), 7.80–7.69 (m, 4H), 7.50 (s, 1H), 6.82 (d, J = 8.99 Hz, 2H), 6.76 (t, J = 7.70, 7.70 Hz, 5H), 3.07 (s, 6H), 3.05 (s, 4H), 2.95 (s, 4H), 2.93 (s, 6H). Exact mass for $\text{C}_{18}\text{H}_{10}\text{F}_6\text{N}_2\text{O}$: 384.0697. HRMS: $[\text{M} + \text{H}]^+$: 385.0790. HPLC1: t_R 5.43 min, purity 95.3%.

(4-Hydroxyphenyl)-(4-(4-hydroxyphenyl)-1H-imidazol-2-yl)-methanone and (4-Hydroxyphenyl)-(5-(4-hydroxyphenyl)-1H-imidazol-2-yl)methanone (11i). ^1H NMR (500 MHz, DMSO- d_6) δ 13.37 (s, 0.37H), 13.29 (s, 1H), 10.39 (s, 1H), 9.46 (s, 1H), 8.60 (d, J = 7.88 Hz, 3H), 8.47 (s, 1H), 7.79 (s, 2H), 7.73 (d, J = 7.48 Hz, 4H), 7.55 (s, 1H), 6.92 (d, J = 8.02 Hz, 4H), 6.81 (d, J = 8.03 Hz, 4H). Exact mass for $\text{C}_{16}\text{H}_{12}\text{N}_2\text{O}_3$: 280.0800. HRMS: $[\text{M} + \text{H}]^+$: 281.0967. HPLC2: t_R 3.54 min, purity 99.8%.

(4-Phenyl-1H-imidazol-2-yl)-(3,4,5-trimethoxyphenyl)methanone and (5-Phenyl-1H-imidazol-2-yl)-(3,4,5-trimethoxyphenyl)-methanone (12a). ^1H NMR (400 MHz, chloroform- d) δ 10.63 (s, 0.48H), 10.47 (s, 1H), 8.19 (s, 2H), 7.98 (s, 1H), 7.82 (t, J = 1.67, 1.67 Hz, 1H), 7.81 (t, J = 1.11, 1.11 Hz, 1H), 7.60–7.53 (m, 1H), 7.51 (d, J = 1.97 Hz, 1H), 7.46–7.30 (m, 3H), 7.29–7.22 (m, 1H), 3.95 (s, 5H), 3.91 (s, 3H), 3.91 (s, 3H), 3.89 (s, 1H). Exact mass for $\text{C}_{19}\text{H}_{18}\text{N}_2\text{O}_4$: 338.1267. HRMS: $[\text{M} + \text{H}]^+$: 339.1423. HPLC2: t_R 6.40 min, purity 95.0%.

(4-(4-Fluorophenyl)-1H-imidazol-2-yl)-(3,4,5-trimethoxyphenyl)-methanone and (5-(4-Fluorophenyl)-1H-imidazol-2-yl)-(3,4,5-trimethoxyphenyl)methanone (12b). ^1H NMR (400 MHz, chloroform- d) δ 10.60 (s, 0.30H), 10.46 (s, 1H), 8.15 (s, 2H), 7.97 (s, 1H), 7.77 (dd, J = 5.35, 8.90 Hz, 2H), 7.58–7.50 (dd, J = 5.10, 8.20 Hz, 0.47 H), 7.48 (s, 0.46 H), 7.46 (s, 1H), 7.45 (s, 1H), 7.10–7.02 (m, 2H), 3.94 (s, 6H), 3.92 (s, 3H), 3.91 (s, 2H), 3.89 (s, 1H). Exact mass for $\text{C}_{19}\text{H}_{17}\text{FN}_2\text{O}_4$: 356.1172. HRMS: $[\text{M} + \text{H}]^+$: 357.1245. HPLC2: t_R 6.90 min, purity 99.3%.

(4-(4-Chlorophenyl)-1H-imidazol-2-yl)-(3,4,5-trimethoxyphenyl)-methanone and (5-(4-Chlorophenyl)-1H-imidazol-2-yl)-(3,4,5-trimethoxyphenyl)methanone (12c). ^1H NMR (400 MHz, chloroform- d) δ 10.57 (s, 0.33H), 10.45 (s, 1H), 8.15 (s, 2H), 7.97 (s, 0.49H), 7.81–7.68 (m, 2H), 7.51–7.47 (m, 1H), 7.36–7.30 (m, 2H), 3.94 (s, 6H), 3.91 (s, 3H), 3.89 (s, 0.75H). Exact mass for $\text{C}_{19}\text{H}_{17}\text{ClN}_2\text{O}_4$: 372.0877. HRMS: $[\text{M} + \text{H}]^+$: 373.0992. HPLC4: t_R 15.76 min, purity 95.6%.

(4-(4-Bromophenyl)-1H-imidazol-2-yl)-(3,4,5-trimethoxyphenyl)-methanone and (5-(4-Bromophenyl)-1H-imidazol-2-yl)-(3,4,5-trimethoxyphenyl)methanone (12d). ^1H NMR (400 MHz, chloroform- d) δ 10.77 (s, 0.36H), 10.59 (s, 1H), 8.24 (s, 2H), 8.06 (s, 1H), 7.78 (d, J = 1.86 Hz, 1H), 7.76 (d, J = 1.98 Hz, 1H), 7.69–7.47 (m, 4H), 4.03 (s, 6H), 4.01 (s, 3H), 4.00 (s, 2H), 3.99 (s, 1H). Exact mass for $\text{C}_{19}\text{H}_{17}\text{BrN}_2\text{O}_4$: 416.0372. HRMS: $[\text{M} + \text{H}]^+$: 417.0496. HPLC1: t_R 6.37 min, purity 96.7%.

(4-(4-(Trifluoromethyl)phenyl)-1H-imidazol-2-yl)-(3,4,5-trimethoxyphenyl)methanone and (5-(4-(Trifluoromethyl)phenyl)-1H-imidazol-2-yl)-(3,4,5-trimethoxyphenyl)methanone (12e). ^1H NMR (400 MHz, chloroform- d) δ 10.90 (s, 0.16H), 10.67 (s, 1H), 8.26 (s, 2H), 8.08 (s, 0.36H), 8.01 (d, J = 7.30 Hz, 2H), 7.80–7.88 (m, 0.79H), 7.76–7.62 (m, 3H), 4.08–3.95 (m, 11H). Exact mass for $\text{C}_{20}\text{H}_{17}\text{F}_3\text{N}_2\text{O}_4$: 406.114. HRMS: $[\text{M} + \text{H}]^+$: 407.1319. HPLC2: t_R 9.60 min, purity 95.1%.

(4-*p*-Tolyl-1*H*-imidazol-2-yl)(3,4,5-trimethoxyphenyl)methanone and (5-*p*-Tolyl-1*H*-imidazol-2-yl)(3,4,5-trimethoxyphenyl)methanone (**12f**). ¹H NMR (400 MHz, chloroform-*d*) δ 10.57 (s, 0.77H), 10.44 (s, 1H), 8.18 (s, 2H), 7.96 (s, 1H), 7.71 (d, *J* = 1.87 Hz, 1H), 7.69 (d, *J* = 1.88 Hz, 1H), 7.47 (d, *J* = 2.44 Hz, 2H), 7.22 (s, 1H), 7.16 (s, 1H), 3.94 (s, 6H), 3.92 (s, 3H), 3.90 (s, 3H), 3.89 (s, 2H). Exact mass for C₂₀H₂₀N₂O₄: 352.1423. HRMS: [M + H]⁺: 353.1527. HPLC1: t_R 5.63 min, purity 95.9%.

(4-(4-Methoxyphenyl)-1*H*-imidazol-2-yl)(3,4,5-trimethoxyphenyl)methanone and (5-(4-Methoxyphenyl)-1*H*-imidazol-2-yl)(3,4,5-trimethoxyphenyl)methanone (**12g**). ¹H NMR (400 MHz, chloroform-*d*) δ 10.60 (s, 1H), 10.50 (s, 1H), 8.27 (s, 2H), 8.05 (s, 1H), 7.84 (s, 1H), 7.82 (s, 1H), 7.59 (d, *J* = 8.87 Hz, 1H), 7.54 (d, *J* = 1.90 Hz, 1H), 7.51 (d, *J* = 2.31 Hz, 1H), 7.05–6.97 (m, 4H), 4.04 (s, 5H), 4.01 (s, 3H), 4.00 (s, 3H), 3.98 (s, 2H), 3.89 (s, 2H), 3.88 (s, 3H). Exact mass for C₂₀H₂₀N₂O₅: 368.1372. HRMS: [M + H]⁺: 369.1572. HPLC4: t_R 13.78 min, purity 96.5%.

(4-(4-(Dimethylamino)phenyl)-1*H*-imidazol-2-yl)(3,4,5-trimethoxyphenyl)methanone and (5-(4-(Dimethylamino)phenyl)-1*H*-imidazol-2-yl)(3,4,5-trimethoxyphenyl)methanone (**12h**). ¹H NMR (500 MHz, chloroform-*d*) δ 10.67 (s, 1H), 10.54 (s, 0.49H), 8.28 (s, 1H), 8.03 (s, 2H), 7.78 (s, 1H), 7.76 (s, 1H), 7.53 (d, *J* = 8.79 Hz, 2H), 7.50 (d, *J* = 1.56 Hz, 1H), 6.78 (m, 4H), 4.03 (s, 4H), 3.99 (s, 8H), 3.97 (s, 3H), 3.04 (s, 6H), 3.02 (s, 4H). Exact mass for C₂₁H₂₃N₃O₄: 381.1689. HRMS: [M + H]⁺: 382.1842. HPLC1: t_R 5.53 min, purity 96.0%.

(4-(4-Hydroxyphenyl)-1*H*-imidazol-2-yl)(3,4,5-trimethoxyphenyl)methanone and (5-(4-Hydroxyphenyl)-1*H*-imidazol-2-yl)(3,4,5-trimethoxyphenyl)methanone (**12i**). ¹H NMR (500 MHz, chloroform-*d*) δ 11.19 (s, 1H), 10.75 (s, 1H), 8.23 (s, 2H), 7.98 (s, 2H), 7.77 (s, 1H), 7.75 (s, 1H), 7.54 (d, *J* = 5.13 Hz, 3H), 7.49 (s, 1H), 6.90 (t, *J* = 9.24, 9.24 Hz, 4H), 4.01 (s, 6H), 3.99 (s, 3H), 3.97 (s, 5H), 3.96 (s, 3H). Exact mass for C₁₉H₁₈N₂O₅: 354.1216. HRMS: [M + H]⁺: 355.1378. HPLC2: t_R 4.46 min, purity 98.1%.

Phenyl(4-(3,4,5-trimethoxyphenyl)-1*H*-imidazol-2-yl)methanone and Phenyl(5-(3,4,5-trimethoxyphenyl)-1*H*-imidazol-2-yl)methanone (**13a**). ¹H NMR (400 MHz, chloroform-*d*) δ 10.67 (s, 1H), 10.51 (s, 1H), 8.68–8.63 (m, 2H), 8.53–8.49 (m, 1H), 7.62–7.53 (m, 2H), 7.53–7.44 (m, 5H), 7.04 (s, 2H), 6.75 (s, 1H), 3.89 (s, 6H), 3.89 (s, 3H), 3.83 (s, 2H), 3.82 (s, 3H). Exact mass for C₁₉H₁₈N₂O₄: 338.1267. HRMS: [M + H]⁺: 339.1348. HPLC2: t_R 5.23 min, purity 97.4%.

(4-Bromophenyl)(4-(3,4,5-trimethoxyphenyl)-1*H*-imidazol-2-yl)methanone and (4-Bromophenyl)(5-(3,4,5-trimethoxyphenyl)-1*H*-imidazol-2-yl)methanone (**13d**). ¹H NMR (400 MHz, chloroform-*d*) δ 10.66 (s, 1H), 10.57 (s, 1H), 8.72–8.62 (m, 2H), 8.56–8.50 (m, 1H), 7.80–7.75 (m, 1H), 7.75–7.67 (m, 4H), 7.57 (q, *J* = 2.04 Hz, 2H), 7.12 (s, 2H), 6.82 (s, 1H), 3.99 (s, 6H), 3.98 (s, 4H), 3.93 (s, 2H), 3.92 (s, 3H). Exact mass for C₁₉H₁₇BrN₂O₄: 416.0372. HRMS: [M + H]⁺: 417.0454. HPLC2: t_R 7.28 min, purity 97.9%.

(4-Methoxyphenyl)(4-(3,4,5-trimethoxyphenyl)-1*H*-imidazol-2-yl)methanone and (4-Methoxyphenyl)(5-(3,4,5-trimethoxyphenyl)-1*H*-imidazol-2-yl)methanone (**13g**). ¹H NMR (400 MHz, chloroform-*d*) δ 10.80 (s, 1H), 10.66 (s, 1H), 8.87–8.79 (m, 2H), 8.73–8.67 (m, 1H), 7.56 (d, *J* = 1.83 Hz, 1H), 7.53 (d, *J* = 2.32 Hz, 1H), 7.14 (s, 2H), 7.05 (dd, *J* = 3.59, 8.90 Hz, 3H), 6.83 (s, 1H), 3.99 (s, 6H), 3.96 (s, 3H), 3.95 (s, 3H), 3.94 (s, 2H), 3.92 (s, 2H), 3.91 (s, 3H). Exact mass for C₂₀H₂₀N₂O₅: 368.1372. HRMS: [M + H]⁺: 369.1494. HPLC2: t_R 5.94 min, purity 97.4%.

(4-(Dimethylamino)phenyl)(4-(3,4,5-trimethoxyphenyl)-1*H*-imidazol-2-yl)methanone and (4-(Dimethylamino)phenyl)(5-(3,4,5-trimethoxyphenyl)-1*H*-imidazol-2-yl)methanone (**13h**). ¹H NMR (400 MHz, chloroform-*d*) δ 11.20 (s, 1H), 10.94 (s, 1H), 8.94–8.75 (m, 2H), 8.74–8.61 (m, 1H), 7.54 (s, 1H), 7.50 (s, 1H), 7.15 (d, *J* = 2.41 Hz, 2H), 6.86 (s, 1H), 6.76 (dd, *J* = 5.30, 9.05 Hz, 3H), 3.99 (s, 7H), 3.93 (s, 4H), 3.91 (s, 6H), 3.14 (s, 6H), 3.13 (s, 4H). Exact mass for C₂₁H₂₃N₃O₄: 381.1689. HRMS: [M + H]⁺: 382.1842. HPLC1: t_R 4.82 min, purity 97.8%.

(4-Hydroxyphenyl)(4-(3,4,5-trimethoxyphenyl)-1*H*-imidazol-2-yl)methanone and (4-Hydroxyphenyl)(5-(3,4,5-trimethoxyphenyl)-1*H*-imidazol-2-yl)methanone (**13i**). ¹H NMR (500 MHz, chloroform-*d*) δ 11.81 (s, 1H), 11.45 (s, 1H), 8.62–8.44 (m, 2H), 8.39–8.19 (m,

2H), 7.53 (d, *J* = 31.95 Hz, 2H), 7.07 (s, 2H), 6.82 (dd, *J* = 12.16, 30.47 Hz, 6H), 3.90 (s, 5H), 3.88 (s, 8H), 3.84 (s, 6H). Exact mass for C₁₉H₁₈N₂O₅: 354.1216. HRMS: [M + H]⁺: 355.1339. HPLC1: t_R 4.00 min, purity 97.4%.

3,4,5-Trimethoxyphenyl-(4-(3,4,5-trimethoxyphenyl)-1*H*-imidazol-2-yl)methanone and 3,4,5-Trimethoxyphenyl-(5-(3,4,5-trimethoxyphenyl)-1*H*-imidazol-2-yl)methanone (**14**). ¹H NMR (400 MHz, chloroform-*d*) δ 10.76 (s, 0.40H), 10.61 (s, 1H), 8.20 (s, 2H), 7.95 (s, 1H), 7.48 (d, *J* = 1.90 Hz, 0.40H), 7.47 (d, *J* = 2.34 Hz, 1H), 7.06 (s, 2H), 6.75 (s, 1H), 3.93 (s, 5H), 3.91 (d, *J* = 0.84 Hz, 4H), 3.89 (s, 1H), 3.87 (s, 2H), 3.86 (s, 5H), 3.83 (s, 1H), 3.82 (s, 2H). Exact mass for C₂₂H₂₄N₂O₇: 428.1584. HRMS: [M + H]⁺: 429.1677. HPLC3: t_R 9.60 min, purity 96.4%.

General Procedure for the Preparation of (4 or 5)-Aryl-2-aryloyl-(1*H*)-imidazole Derivatives (15a–c**).** To a solution of **12a** (135 mg, 0.4 mmol) in THF (10 mL) in ice-bath was added sodium hydride (60% dispersion in mineral oil, 28 mg, 0.60 mmol) followed by adding methyl iodide (85 mg, 0.60 mmol) (for **15a**) or ethyl iodide (93 mg, 0.60 mmol) (for **15b**) or benzyl bromide (102 mg, 0.60 mmol) (for **15c**). The resulting reaction mixture was stirred overnight under reflux condition. After dilution by 50 mL of saturated NaHCO₃ solution (aqueous), the reaction mixture was extracted by ethyl acetate (100 mL). The organic layer was dried over magnesium sulfate and concentrated. The residue was purified by flash column chromatography.

(1-Methyl-4-phenyl-1*H*-imidazol-2-yl)(3,4,5-trimethoxyphenyl)methanone (**15a**). ¹H NMR (500 MHz, chloroform-*d*) δ 7.97 (d, *J* = 2.38 Hz, 2H), 7.85 (d, *J* = 6.01 Hz, 2H), 7.46–7.39 (m, 3H), 7.28 (d, *J* = 2.39 Hz, 1H), 4.16–4.10 (m, 3H), 3.99 (d, *J* = 2.82 Hz, 9H). Exact mass for C₂₀H₂₀N₂O₄: 352.1423. HRMS: [M + H]⁺: 353.1527. HPLC1: t_R 6.03 min, purity 96.4%.

(1-Ethyl-4-phenyl-1*H*-imidazol-2-yl)(3,4,5-trimethoxyphenyl)methanone (**15b**). ¹H NMR (400 MHz, chloroform-*d*) δ 7.95 (s, 2H), 7.89–7.83 (m, 2H), 7.51 (s, 1H), 7.43 (t, *J* = 7.61, 7.61 Hz, 2H), 7.36–7.31 (m, 1H), 4.56 (q, *J* = 7.19, 7.19, 7.19 Hz, 2H), 3.99 (s, 6H), 3.98 (s, 3H), 1.30 (t, *J* = 7.19, 7.19 Hz, 3H). Exact mass for C₂₁H₂₂N₂O₄: 366.158. HRMS: [M + H]⁺: 367.1725. HPLC1: t_R 6.47 min, purity 97.1%.

(1-Benzyl-4-phenyl-1*H*-imidazol-2-yl)(3,4,5-trimethoxyphenyl)methanone (**15c**). ¹H NMR (500 MHz, chloroform-*d*) δ 7.94 (d, *J* = 1.70 Hz, 2H), 7.84 (d, *J* = 7.73 Hz, 2H), 7.47–7.28 (m, 9H), 5.74 (s, 2H), 3.98 (s, 9H). Exact mass for C₂₆H₂₄N₂O₄: 428.1736. HRMS: [M + H]⁺: 429.1931. HPLC1: t_R 6.70 min, purity 95.4%.

General Procedure for the Preparation of (4 or 5)-Aryl-2-aryloyl-(1*H*)-imidazole Derivatives (15d–f**).** To a solution of **12a** (135 mg, 0.4 mmol) in ACN (10 mL) was added potassium carbonate (82 mg, 0.60 mmol) followed by *n*-propyl iodide (82 mg, 0.48 mmol) (for **15d**) or *i*-propyl iodide (82 mg, 0.48 mmol) (for **15e**) or cyclopentyl bromide (72 mg, 0.48 mmol) (for **15f**). The resulting reaction mixture was stirred overnight under reflux condition. After dilution by 50 mL of saturated NaHCO₃ solution (aqueous), the reaction mixture was extracted by ethyl acetate (100 mL). The organic layer was dried over magnesium sulfate and concentrated. The residue was purified by flash column chromatography.

(4-Phenyl-1-propyl-1*H*-imidazol-2-yl)(3,4,5-trimethoxyphenyl)methanone (**15d**). ¹H NMR (500 MHz, chloroform-*d*) δ 7.94 (s, 2H), 7.90–7.82 (m, 2H), 7.47 (s, 1H), 7.42 (t, *J* = 7.67 Hz, 2H), 7.34–7.28 (m, 1H), 4.51–4.40 (m, 2H), 3.98 (d, *J* = 1.49 Hz, 9H), 1.96 (h, *J* = 7.40 Hz, 2H), 1.03 (t, *J* = 7.42 Hz, 3H). Exact mass for C₂₂H₂₄N₂O₄: 380.1700. HRMS: [M + H]⁺: 381.1897. HPLC1: t_R 6.88 min, purity 98.0%.

(1-Isopropyl-4-phenyl-1*H*-imidazol-2-yl)(3,4,5-trimethoxyphenyl)methanone (**15e**). ¹H NMR (400 MHz, chloroform-*d*) δ 7.79 (s, 3H), 7.78–7.73 (m, 1H), 7.57 (s, 1H), 7.34 (dd, *J* = 6.87, 8.44 Hz, 2H), 7.25–7.21 (m, 1H), 5.66–5.21 (m, 1H), 3.89 (s, 9H), 1.52 (s, 6H). Exact mass for C₂₂H₂₄N₂O₄: 380.1700. HRMS: [M + H]⁺: 381.1937. HPLC1: t_R 6.90 min, purity 98.3%.

(1-Cyclopentyl-4-phenyl-1*H*-imidazol-2-yl)(3,4,5-trimethoxyphenyl)methanone (**15f**). ¹H NMR (500 MHz, chloroform-*d*) δ 7.90–7.82 (m, 4H), 7.61 (d, *J* = 1.7 Hz, 1H), 7.42 (td, *J* = 7.7, 1.7 Hz, 2H), 7.33–7.28 (m, 1H), 5.88–5.32 (m, 1H), 3.98 (t, *J* =

1.9 Hz, 9H), 2.64–2.20 (m, 2H), 2.00–1.77 (m, 6H). Exact mass for $C_{24}H_{26}N_2O_4$: 406.1893. HRMS: $[M + H]^+$: 407.2103. HPLC1: t_R 8.07 min, purity 98.3%.

General Procedure for the Preparation of (4 or 5)-Aryl-2-aryloyl-(1H)-imidazole Derivatives (15g–h). Under inert atmosphere, a Schlenk flask was charged with CS_2CO_3 (260 mg, 0.8 mmol), CuI (76 mg, 0.4 mmol), ligand (0.4 mmol), compound 12a (135 mg, 0.4 mmol), 2-pyrimidyl bromide (124 mg, 0.8 mmol) (for 15g), or 2-bromothiophene (130 mg, 0.8 mmol) (for 15h) and DMF (5 mL). The reaction mixture was stirred for 30 min at room temperature and then heated to 110 °C for 2 days. The reaction mixture was monitored by TLC. After the starting material was completely consumed, the reaction was stopped and the mixture was cooled to room temperature. The reaction mixture was directly passed through a plug of silica gel. After being rinsed with ethyl acetate, the combined filtrate was washed with saturated brine. After the organic layer was dried by sodium sulfate, it was concentrated. The residue was purified by column chromatography on silica gel to provide the desired product.

(4-Phenyl-1-(pyridin-2-yl)-1H-imidazol-2-yl)(3,4,5-trimethoxyphenyl)methanone (15g). 1H NMR (500 MHz, chloroform- d) δ 8.59 (dt, J = 1.70, 4.33 Hz, 1H), 7.91 (ddt, J = 1.67, 3.99, 7.42 Hz, 3H), 7.86 (d, J = 1.52 Hz, 2H), 7.82 (d, J = 1.57 Hz, 1H), 7.48–7.40 (m, 4H), 7.34 (td, J = 1.38, 7.27 Hz, 1H), 3.98 (d, J = 1.62 Hz, 3H), 3.96 (d, J = 1.41 Hz, 6H). Exact mass for $C_{24}H_{21}N_3O_4$: 415.1500. HRMS: $[M + H]^+$: 416.1692. HPLC1: t_R 4.85 min, purity, 97.9%.

(4-Phenyl-1-(thiophen-2-yl)-1H-imidazol-2-yl)(3,4,5-trimethoxyphenyl)methanone (15h). 1H NMR (500 MHz, chloroform- d) δ 7.87–7.76 (m, 4H), 7.52 (d, J = 1.84 Hz, 1H), 7.37 (td, J = 1.83, 7.63, 8.06 Hz, 2H), 7.30–7.23 (m, 2H), 7.06 (dd, J = 1.95, 3.59 Hz, 1H), 6.97 (dp, J = 1.70, 5.60 Hz, 1H), 3.89 (d, J = 1.94 Hz, 3H), 3.88 (d, J = 1.95 Hz, 6H). Exact mass for $C_{23}H_{20}N_2O_4S$: 420.1100. HRMS: $[M + H]^+$: 421.1298. HPLC1: t_R 6.33 min, purity 98.2%.

General Procedure for the Preparation of (4 or 5)-Alkyl-(5 or 4)-aryl-2-aryloyl-(1H)-imidazole Derivatives (18a–c). To ammonium acetate (10 mmol) in ethanol (5 mL) and water (0.3 mL) was added phenyl alkyl diones 17(a–c) (1 mmol) in ethanol (5 mL) and 3,4,5-trimethoxyphenyl glyoxal hydrate 10 (1 mmol) in ethanol (10 mL). The mixture was stirred at room temperature for 30–45 min. The reaction was stopped after the consumption of the starting material monitored by TLC. The mixture was then extracted with ethyl acetate. The organic layer was washed with brine, dried over anhydrous sodium sulfate, and concentrated to get the crude product. The crude was purified by flash chromatography.

(5-Methyl-4-phenyl-1H-imidazol-2-yl)(3,4,5-trimethoxyphenyl)methanone and (4-Methyl-5-phenyl-1H-imidazol-2-yl)(3,4,5-trimethoxyphenyl)methanone (18a). 1H NMR (400 MHz, chloroform- d) δ 10.43 (s, 0.59H), 10.32 (s, 1H), 8.24 (s, 2H), 8.05 (s, 1H), 7.87–7.71 (m, 3H), 7.62–7.38 (m, 6H), 4.02 (s, 5H), 4.01 (s, 3H), 3.99 (s, 2H), 3.98 (s, 2H), 3.95 (s, 2H), 2.64 (s, 3H), 2.56 (s, 1H). Exact mass for $C_{19}H_{17}ClN_2O_4$: 372.0877. HRMS: $[M + H]^+$: 373.0992. HPLC2: t_R 6.42 min, purity 95.4%.

(5-Ethyl-4-phenyl-1H-imidazol-2-yl)(3,4,5-trimethoxyphenyl)methanone and (4-Ethyl-5-phenyl-1H-imidazol-2-yl)(3,4,5-trimethoxyphenyl)methanone (18b). 1H NMR (400 MHz, chloroform- d) δ 10.85 (s, 1H), 8.28 (s, 2H), 8.15 (s, 1H), 7.75 (m, 1H), 7.45–7.30 (m, 5H), 4.00 (m, 9H), 3.05 (m, 2H), 1.40 (m, 3H). Exact mass for $C_{19}H_{17}ClN_2O_4$: 372.0877. HRMS: $[M + H]^+$: 373.0992. HPLC1: t_R 5.37 min, purity 96.3%.

(4-Phenyl-5-propyl-1H-imidazol-2-yl)(3,4,5-trimethoxyphenyl)methanone and (5-Phenyl-4-propyl-1H-imidazol-2-yl)(3,4,5-trimethoxyphenyl)methanone (18c). 1H NMR (400 MHz, chloroform- d) δ 10.52 (s, 0.52 H), 10.47 (s, 1H), 8.24 (s, 2H), 8.14 (s, 1H), 7.78 (d, J = 7.39 Hz, 2H), 7.60–7.43 (m, 5H), 7.36 (t, J = 7.40, 7.40 Hz, 1H), 4.01 (s, 5H), 4.00 (s, 3H), 3.99 (s, 4H), 3.00–2.93 (t, J = 7.40, 7.40 Hz, 2H), 2.84 (t, J = 7.50, 7.50 Hz, 1H), 1.94–1.87 (m, 1H), 1.87–1.78 (m, 2H), 1.07 (t, J = 7.33, 7.33 Hz, 3H), 0.98–0.92 (t, J = 7.10, 7.10 Hz, 1H). Exact mass for $C_{19}H_{17}ClN_2O_4$: 372.0877. HRMS: $[M + H]^+$: 373.0992. HPLC: t_R 12.46 min, purity 96.1%.

Cell Culture and Cytotoxicity Assay. We examined the antiproliferative activity of the RABI compounds in four human melanoma cell lines (A375 and WM-164, MDA-MB-435, and MDA-MB-435/LCC6MDR1) and four human prostate cancer cell lines (LNCaP, DU 145, PC-3, and PPC-1). All these cell lines were purchased from ATCC (American Type Culture Collection, Manassas, VA). Melanoma cells were cultured in DMEM (Cellgro Mediatech Inc., Herndon, VA), and prostate cancer cells were cultured in RPMI 1640 (Cellgro Mediatech, Inc., Herndon, VA) supplemented with 10% fetal bovine serum (Cellgro Mediatech). Cultures were maintained at 37 °C in a humidified atmosphere containing 5% CO_2 . Then 1000–5000 cells were plated into each well of 96-well plates depending on growth rate and exposed to different concentrations of a test compound for 48 h (fast growing melanoma cells) or 96 h (slow growing prostate cancer cells) in three–five replicates. Cell numbers at the end of the drug treatment were measured by the sulforhodamine B (SRB) assay. Briefly, the cells were fixed with 10% trichloroacetic acid and stained with 0.4% SRB, and the absorbances at 540 nm were measured using a plate reader (DYNEX Technologies, Chantilly VA). Percentages of cell survival versus drug concentrations were plotted, and the IC_{50} (concentration that inhibited cell growth by 50% of untreated control) values were obtained by nonlinear regression analysis using GraphPad Prism (GraphPad Software, San Diego, CA).

Cell Cycle Analysis. Cell cycle distribution was determined by propidium iodide (PI) staining. Treated cells were washed with PBS and fixed with 70% ice-cold ethanol overnight. Fixed cells were then stained with 20 μ g/mL of PI in the presence of RNase A (300 μ g/mL) at 37 °C for 30 min. Cell cycle distribution was analyzed by fluorescence-activated cell sorting (FACS) analysis core services at the University of Tennessee Health Science Center, TN.

Molecular Modeling. All molecular modeling studies were performed with Schrodinger Molecular Modeling Suite 2011 (Schrodinger LLC, New York, NY) running on a Dell Linux workstation. We selected tubulin complex with TN16 (PDB code: 3HKD) and tubulin complex with colchicine (PDB code: 1SA0) as our modeling system. RABIs were built and prepared using the Ligprep module, and they were docked into the TN16 site and colchicine site by the Glide module in the Schrodinger Suite. The best docking complexes were subject to restricted molecular dynamics to release any strains by using the MacroModel module with OPLS-2005 force field. The ligand and its surrounding residues within 15 Å were allowed to move freely, while the outer atoms are frozen.

■ ASSOCIATED CONTENT

● Supporting Information

Structure elucidation of 12a; in vitro tubulin polymerization assay; competitive binding at the colchicine site in tubulin for compounds 12a and 15g. This material is available free of charge via the Internet at <http://pubs.acs.org>.

■ AUTHOR INFORMATION

Corresponding Author

*Phone: (901)448-7532. Fax: (901)448-6828. E-mail: wli@uthsc.edu.

Author Contributions

[§]These authors contributed equally.

Notes

The authors declare no competing financial interest.

■ ACKNOWLEDGMENTS

This work was supported by the NIH grants R01CA148706, 1S10RR026377-01, and 1S10OD010678-01 and funds from GTx, Inc. The content is solely the responsibility of the authors and does not necessarily represent the official views of the National Institutes of Health.

■ ABBREVIATIONS USED

ABI, 2-aryl-4-benzoyl-imidazoles; RABI, reverse ABI; HMBC, heteronuclear multiple-bond correlation spectroscopy; Pgp, P-glycoprotein; SAR, structure–activity relationship; ND, not determined; PI, propidium iodide; FACS, fluorescence-activated cell sorting; SRB, sulforhodamine B

■ REFERENCES

- (1) Jemal, A.; Bray, F.; Center, M. M.; Ferlay, J.; Ward, E.; Forman, D. Global cancer statistics. *CA—Cancer J. Clin.* **2011**, *61* (2), 69–90.
- (2) Siegel, R.; Naishadham, D.; Jemal, A. Cancer statistics, 2012. *CA—Cancer J. Clin.* **2012**, *62* (1), 10–29.
- (3) Chen, J.; Wang, Z.; Li, C. M.; Lu, Y.; Vaddady, P. K.; Meibohm, B.; Dalton, J. T.; Miller, D. D.; Li, W. Discovery of novel 2-aryl-4-benzoyl-imidazoles targeting the colchicines binding site in tubulin as potential anticancer agents. *J. Med. Chem.* **2010**, *53* (20), 7414–7427.
- (4) Chen, J.; Ahn, S.; Wang, J.; Lu, Y.; Dalton, J. T.; Miller, D. D.; Li, W. Discovery of novel 2-aryl-4-benzoyl-imidazole (ABI-III) analogues targeting tubulin polymerization as antiproliferative agents. *J. Med. Chem.* **2012**, *55* (16), 7285–7289.
- (5) Li, C. M.; Lu, Y.; Chen, J.; Costello, T. A.; Narayanan, R.; Dalton, M. N.; Snyder, L. M.; Ahn, S.; Li, W.; Miller, D. D.; Dalton, J. T. Orally bioavailable tubulin antagonists for paclitaxel-refractory cancer. *Pharm. Res.* **2012**, *29* (11), 3053–3063.
- (6) Wang, Z.; Chen, J.; Wang, J.; Ahn, S.; Li, C. M.; Lu, Y.; Loveless, V. S.; Dalton, J. T.; Miller, D. D.; Li, W. Novel tubulin polymerization inhibitors overcome multidrug resistance and reduce melanoma lung metastasis. *Pharm. Res.* **2012**, *29* (11), 3040–3052.
- (7) Chen, J.; Li, C. M.; Wang, J.; Ahn, S.; Wang, Z.; Lu, Y.; Dalton, J. T.; Miller, D. D.; Li, W. Synthesis and antiproliferative activity of novel 2-aryl-4-benzoyl-imidazole derivatives targeting tubulin polymerization. *Bioorg. Med. Chem.* **2011**, *19* (16), 4782–4795.
- (8) Li, C. M.; Chen, J.; Lu, Y.; Narayanan, R.; Parke, D. N.; Li, W.; Ahn, S.; Miller, D. D.; Dalton, J. T. Pharmacokinetic optimization of 4-substituted methoxybenzoyl-aryl-thiazole and 2-aryl-4-benzoyl-imidazole for improving oral bioavailability. *Drug Metab. Dispos.* **2011**, *39* (10), 1833–1839.
- (9) Khalili, B.; Tondro, T.; Hashemi, M. M. Novel one-pot synthesis of (4 or 5)-aryl-2-aryloyl-(1H)-imidazoles in water and tautomerization study using NMR. *Tetrahedron* **2009**, *65* (34), 6882–6887.
- (10) Parkinson, E. I.; Jason Hatfield, M.; Tsurkan, L.; Hyatt, J. L.; Edwards, C. C.; Hicks, L. D.; Yan, B.; Potter, P. M. Requirements for mammalian carboxylesterase inhibition by substituted ethane-1,2-diones. *Bioorg. Med. Chem.* **2011**, *19* (15), 4635–4643.
- (11) Pelphe, P. M.; Popov, V. M.; Joska, T. M.; Beierlein, J. M.; Bolstad, E. S.; Fillingham, Y. A.; Wright, D. L.; Anderson, A. C. Highly efficient ligands for dihydrofolate reductase from *Cryptosporidium hominis* and *Toxoplasma gondii* inspired by structural analysis. *J. Med. Chem.* **2007**, *50* (5), 940–950.
- (12) Riley, H. A.; Gray, A. R. General procedure for synthesis of glyoxal derivatives. In *Organic Syntheses*; Wiley & Sons: New York, NY, 1943; Vol. 2, pp 509–510.
- (13) Corelli, F.; Summa, V.; Brogi, A.; Monteagudo, E.; Botta, M. Chiral Azole Derivatives 0.2. Synthesis of Enantiomerically Pure 1-Alkylimidazoles. *J. Org. Chem.* **1995**, *60* (7), 2008–2015.
- (14) Sabbah, M.; Souler, L.; Reverchon, S.; Queneau, Y.; Doutheau, A. LuxR dependent quorum sensing inhibition by *N,N'*-disubstituted imidazolium salts. *Bioorg. Med. Chem.* **2011**, *19* (16), 4868–4875.
- (15) Xi, Z. X.; Liu, F. H.; Zhou, Y. B.; Chen, W. Z. CuI/L (L = pyridine-functionalized 1,3-diketones) catalyzed C–N coupling reactions of aryl halides with NH-containing heterocycles. *Tetrahedron* **2008**, *64* (19), 4254–4259.
- (16) Lu, Y.; Li, C. M.; Wang, Z.; Ross, C. R., II; Chen, J.; Dalton, J. T.; Li, W.; Miller, D. D. Discovery of 4-substituted methoxybenzoyl-aryl-thiazole as novel anticancer agents: synthesis, biological evaluation, and structure–activity relationships. *J. Med. Chem.* **2009**, *52* (6), 1701–1711.
- (17) Leonessa, F.; Green, D.; Licht, T.; Wright, A.; Wingate-Legette, K.; Lippman, J.; Gottesman, M. M.; Clarke, R. MDA435/LCC6 and MDA435/LCC6MDR1: ascites models of human breast cancer. *Br. J. Cancer* **1996**, *73* (2), 154–161.
- (18) Vredenburg, M. R.; Ojima, I.; Veith, J.; Pera, P.; Kee, K.; Cabral, F.; Sharma, A.; Kanter, P.; Greco, W. R.; Bernacki, R. J. Effects of orally active taxanes on P-glycoprotein modulation and colon and breast carcinoma drug resistance. *J. Natl. Cancer Inst.* **2001**, *93* (16), 1234–1245.
- (19) Zhang, S.; Morris, M. E. Effects of the flavonoids biochanin A, morin, phloretin, and silymarin on P-glycoprotein-mediated transport. *J. Pharmacol. Exp. Ther.* **2003**, *304* (3), 1258–1267.
- (20) Dong, X.; Mattingly, C. A.; Tseng, M. T.; Cho, M. J.; Liu, Y.; Adams, V. R.; Mumper, R. J. Doxorubicin and paclitaxel-loaded lipid-based nanoparticles overcome multidrug resistance by inhibiting P-glycoprotein and depleting ATP. *Cancer Res.* **2009**, *69* (9), 3918–3926.
- (21) Barbier, P.; Dorleans, A.; Devred, F.; Sanz, L.; Allegro, D.; Alfonso, C.; Knossow, M.; Peyrot, V.; Andreu, J. M. Stathmin and interfacial microtubule inhibitors recognize a naturally curved conformation of tubulin dimers. *J. Biol. Chem.* **2010**, *285* (41), 31672–31681.
- (22) Dorleans, A.; Gigant, B.; Ravelli, R. B.; Mailliet, P.; Mikol, V.; Knossow, M. Variations in the colchicine-binding domain provide insight into the structural switch of tubulin. *Proc. Natl. Acad. Sci. U. S. A.* **2009**, *106* (33), 13775–13779.